Aging of Polyethylene Pipes Transporting Drinking Water Disinfected by Chlorine Dioxide. I. Chemical Aspects

X. Colin,[1] L. Audouin,[1] J. Verdu,[1] M. Rozental-Evesque,[2] B. Rabaud,[2] F. Martin,[3] F. Bourgine[4]
[1] *Arts et Métiers ParisTech, LIM, 75013 Paris, France*

[2] *Suez-Environnement, Cirsee, 78230 Le Pecq, France*

[3] *Veolia-Environnement, Anjou Recherche, 78603 Maisons Laffitte, France*

[4] *Saur Direction Métiers, Les Cyclades, 78064 Saint-Quentin-en-Yvelines Cedex, France*

Aging of unfilled polyethylene (PE) films in concentrated (80–100 ppm) chlorine dioxide (DOC) solutions at 20°C and 40 has been studied by IR spectrophotometry, melt rheometry, chlorine titration, and tensile testing to establish the mechanisms of PE degradation induced by DOC, to determine some important kinetic parameters, to identify the embrittlement mechanism, and to examine the possibility to predict nonempirically embrittlement from a kinetic model. Experimental results reveal that DOC initiates PE oxidation. This latter is responsible for hydroperoxide build-up, and chain scissions occur when hydroperoxides reach a critical concentration above which they decompose bimolecularly. The weight average molar mass M_w decreases and embrittlement occurs when M_w approaches a value of 70 kg mol^{-1} as previously found in thermooxidation studies. A mechanistic scheme involving all the elementary steps of PE autooxidation plus one initiation and one termination step involving DOC has been elaborated. The kinetic scheme derived from this mechanistic scheme has been solved numerically and the results of simulations have been compared with experimental results. POLYM. ENG. SCI., 49:1429–1437, 2009. © 2009 Society of Plastics Engineers

INTRODUCTION

It is well known that the polyethylene (PE) pipes containing pressurized water undergo failure after a time t_F which is a decreasing function of pressure p and temperature T. Laboratory isothermal, isobaric experiments aimed to establish the dependence of t_F with T and p, are usually translated into ($\log \sigma - \log t_F$) graphs, σ being the hoop stress. International standards, starting from the observation that, in certain (σ, t_F) domains, these plots are quasi linear, propose to characterize the material by the equations of the corresponding straightlines [NFT 54091 (AFNOR)]. In the case of polyethylenes used until the beginning of this century (the last PE generation: PE100 will not be considered here), three kinetic regimes corresponding to three distinct straight lines in the ($\log \sigma - \log t_F$) graph were distinguished [1–3]. Regime I, at high stresses and low lifetimes, is characterized by a low slope: $d(\log \sigma)/d(\log t_F) \sim 0.03$ and by a ductile fracture. Regime II, at lower stresses, is characterized by a higher slope: $d(\log \sigma)/d(\log t_F) \sim 0.3$ and by a brittle fracture. Regime III, at low stresses, is also characterized by a brittle fracture, but the slope is higher than in regime II. The difference between Regimes II and III can be established from molar mass measurements. The molar mass distribution is not affected in Regime II, whereas it is shifted toward low values in Regime III. In other words, Regimes I and II are modes of "physical aging," whereas Regime III is a mode of chemical aging. Regimes II and III are in competition. If chemical degradation is fast enough, Regime II totally disappears (see Fig. 1).

Water is not reactive with PE, but it contains generally two reactive species: oxygen and disinfectants. PE autoxidation is very slow at low temperature, typically $T \leq 80$°C, but it can become significant in a timescale comparable with the transition between Regimes I and II, at higher temperatures. Aging of PE tubes under pressure in hot water has been extensively studied by a Swedish group [3–6]. In the temperature range under investigation ($T \geq 90$°C), the pipe durability seems to be governed by the antioxidant migration [3–6]. At lower temperatures,

Correspondence to: X. Colin; e-mail: xavier.colin@paris.ensam.fr
DOI 10.1002/pen.21258
Published online in Wiley InterScience (www.interscience.wiley.com).
© 2009 Society of Plastics Engineers

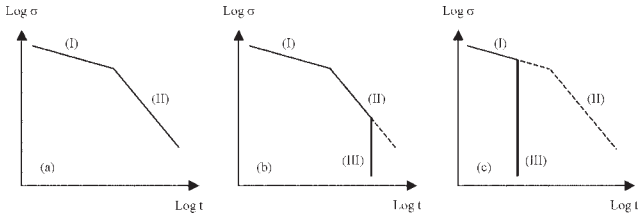

FIG. 1. Shape of (log σ − log t_F) graphs according to Refs. [1–3].

however, the "oxidation lifetime" becomes longer than the "physical aging" lifetime and Regime II becomes (in the absence of disinfectants) the predominant failure mode. Disinfectants, especially chlorine derivatives, are known to destroy organic compounds, often by radical processes. PE does not display an especially high radical reactivity, but zero reactivity would be surprising, because radical reactions are never totally selective. Furthermore, PE contains antioxidants, among which phenols are highly reactive in radical processes. Disinfectants are thus expected to have a deleterious effect on PE pipe durability, at least from their destabilizing effect. This latter has been clearly put in evidence from experimentally established stabilizer concentration profiles. The stabilizer is consumed more rapidly in the presence than in the absence of disinfectant in water, at least in a superficial layer at the water–polymer interface [7, 8]. Which is the embrittlement mechanism in this case? Is the disinfectant-PE reaction negligible or not? Which is the role of oxidation? How to predict embrittlement and fracture times in this case?

The present article is aimed to try to answer the above questions in the case where the disinfectant is chlorine dioxide (DOC). In a first part, DOC-PE reactions will be studied in controlled conditions, to establish the main degradation mechanisms and the corresponding kinetic parameters. Unfilled PE films will be used in this study to avoid analytical problems due to degradation profiles (diffusion controlled processes) and to the presence of carbon black. The second part will be devoted to the study of degradation profiles in pipes exposed to accelerated or natural aging and the coupling between the stress state and the chemical degradation, to try to predict failure.

EXPERIMENTAL

Material

The PE sample under study was obtained from metallocene catalyzed polymerization and presents the following characteristics: weight average molar mass: M_w = 109 kg mol^{-1}; polydispersity index: $I_p \approx 2$; density: ρ = 0.934; melting point: T_m = 129.3°C; crystallinity ratio: $X_C \approx 45\%$. Unsaturations are almost undetectable in transmission IR spectra of films under investigation. However, measurements on thicker samples revealed the presence of vinyl (910 cm^{-1}) and trans-vinylene (966 cm^{-1}) double bonds. The overall unsaturation concentration estimated from band absorbances was about 11 × 10^{-3} mol l^{-1} against about 60 mol l^{-1} for methylenes. Despite the fact that double bonds are more reactive than methylenes (in polymethylenic sequences) toward oxidation, it has been previously checked, experimentally and from model simulations, that, such a low concentration plays a negligible role in the whole oxidation kinetics.

The PE sample contained also an antioxidant which was not identified. As it will be shown in the second part of this article, the antioxidant is rapidly consumed and plays a negligible role on polymer oxidation kinetics, especially in the accelerated aging conditions under study.

Films of 100 ± 30 μm thickness were compression molded at 180°C under 3 MPa pressure. Two types of samples were cut from the films: dogbone samples of 22 mm calibrated length for tensile testing and 25 × 25 mm squares for physicochemical testing.

Aging Tests

The PE samples were immersed in 80–90 ppm DOC solutions at 20°C or 40°C with two distinct pH values: 2–3 and 6. DOC was periodically titrated and its concentration readjusted at its initial value.

DOC solutions were produced by reaction of chlorite anion with chlorydric acid in stoechiometric excess. The global reaction can be summarized as follows:

$$5NaClO_2 + 4HCl \rightarrow 4ClO_2 + 5NaCl + 2H_2O.$$

The excess of chlorydric acid increases the reaction yield.

Sample Characterization

Tensile testing was made on an INSTRON 4301 machine at 23°C, 50% RH, at a 7.5 × 10^{-3} s^{-1} strain rate. IR spectrophotometry (Bruker IFS 28) was used in transmittance mode to determine the absorbance of the carbonyl peak at ~1720 cm^{-1}. The carbonyl concentration was determined using the Beer-Lambert law with a molar absorptivity of 200 l mol^{-1} cm^{-1}. Rheometry (Rheometrics ARES) was used to record the viscosity-angular frequency curves at 160°C in nitrogen atmosphere. Examples of such curves are shown in Fig. 2. The viscosity at the Newtonian plateau η_0 first increases slightly and then, decreases continuously. The average molar mass M_W was determined from the universal scaling law:

$$\eta_0 = KM_w^{3.4}, \quad (1)$$

taking $K = 2.46 \times 10^{-4}$ Pa s mol$^{3.4}$ kg$^{-3.4}$

DOI 10.1002/pen

15482634, 2009, 7, Downloaded from https://4spepublications.onlinelibrary.wiley.com/doi/10.1002/pen.21258 by ENSAM, Wiley Online Library on [09/04/2025]. See the Terms and Conditions (https://onlinelibrary.wiley.com/terms-and-conditions) on Wiley Online Library for rules of use; OA articles are governed by the applicable Creative Commons License

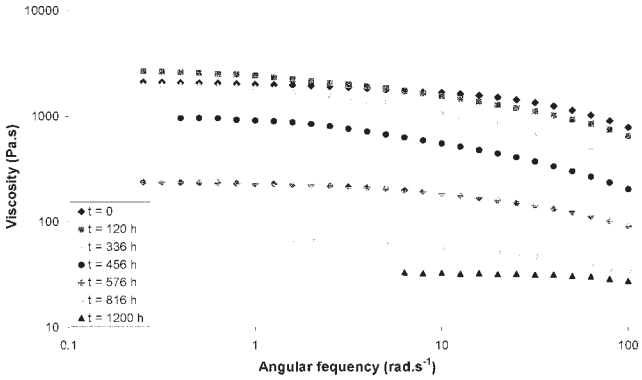

FIG. 2. Examples of viscosity versus angular frequency curves of PE films after immersion in a ~80 ppm DOC solution at 40°C and pH = 2–3.

The number of chain scissions s and crosslinks x par mass unit are given by [9]:

$$\frac{1}{M_n} - \frac{1}{M_{n0}} = s - x \tag{2}$$

$$\frac{1}{M_w} - \frac{1}{M_{w0}} = \frac{s}{2} - 2x \tag{3}$$

Chlorine grafted to the polymer was titrated by elemental analysis. Samples of 1–2 mg in weight were exposed in a mixture of He/O_2 gases at 1050°C. Volatile degradation products were separated by a chromatographic column and detected by a catharometer. The detection limit of Cl by this technique is 0.20% in weight.

RESULTS

Embrittlement

Examples of tensile curves are shown in Fig. 3. The yield stress remains almost constant within experimental scatter: $\sigma_y = 13 \pm 3$ MPa. In contrast, the ultimate strain ε_R first increases slightly and then decreases continuously (see Fig. 4). Taking arbitrarily $\varepsilon_R = 100\%$ as an embrittlement criterion, one finds an embrittlement time of about 500 h at 40°C. The samples keep some ductility after 1200 h at 20°C. Embrittlement appears as practically pH independent.

Oxidation Products

Examples of IR spectra are shown in Fig. 5. Bands grow at 3300–3500 cm^{-1} (hydroxyls) and at 1680–1750 cm^{-1} (carbonyls). Carbonyl build-up kinetic curves are shown in Fig. 6. Carbonyl growth is faster at 40°C than at 20°C and practically pH independent.

Molar Mass Changes

Weight average molar mass M_W determined from rheometric measurements was plotted against exposure time in Fig. 7. At 40°C M_w increases slightly in the early days of exposure, and then decreases continuously to reach 20–30% of its initial value after 1200 h. At 20°C, M_W also increases slightly in the early days of exposure, but its further change is too small to be measurable, so that M_W (1200 h) is practically equal to its initial value within experimental incertitudes.

Chlorine Content

Chlorine is grafted to the polymer. Its concentration increases almost linearly with exposure time (see Fig. 8) to reach a value of the order of 0.22 mol l^{-1} at 40°C and 0.11 mol l^{-1} at 20°C, after 1200 h.

DISCUSSION

Chlorine dioxide is a free radical in ground state:

O═Cl—O°.

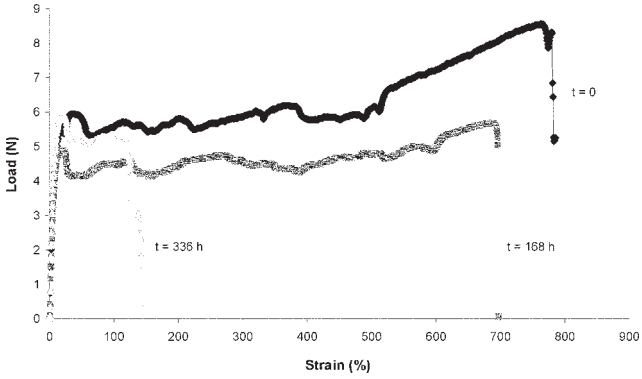

FIG. 3. Examples of tensile curves of PE films after immersion in a ~80 ppm DOC solution at 40°C and pH = 2–3.

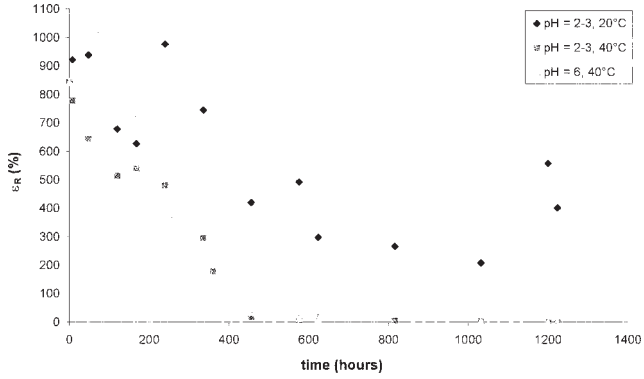

FIG. 4. Kinetic curves of ultimate strain of PE films after immersion in 80–90 ppm DOC solutions at 20 or 40°C and pH = 2–3 or 6.

15482634, 2009, 7, Downloaded from https://4spepublications.onlinelibrary.wiley.com/doi/10.1002/pen.21258 by ENSAM, Wiley Online Library on [09/04/2025]. See the Terms and Conditions (https://onlinelibrary.wiley.com/terms-and-conditions) on Wiley Online Library for rules of use; OA articles are governed by the applicable Creative Commons License

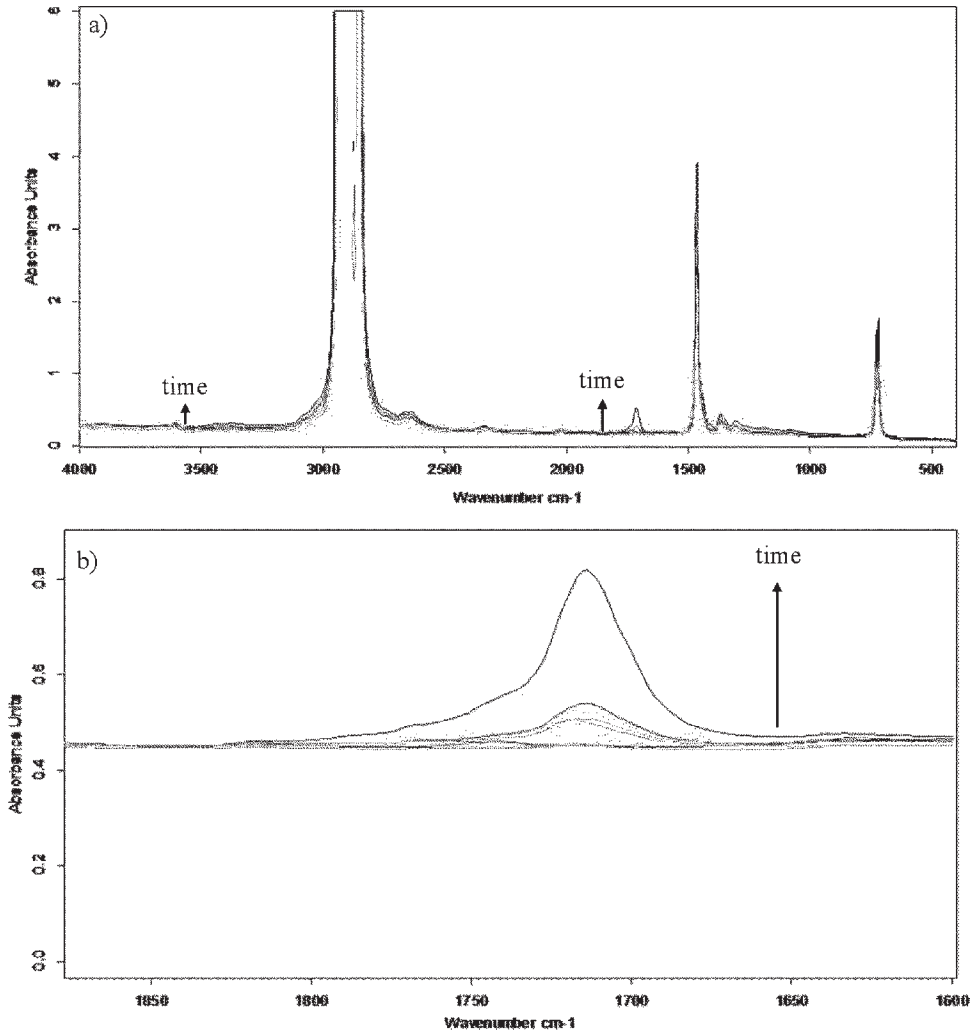

FIG. 5. Examples of IR spectra of PE films after immersion in a ~80 ppm DOC solution at 40°C and pH = 6. (a) Entire IR spectra; (b) Enlargement around the carbonyl band region.

As a nonionic (moderately polar) species, it is slightly soluble in PE. Kinetic modeling needs the knowledge of its solubility, i.e., of the relationship existing between its equilibrium concentration in PE and its concentration in water. An indirect approach based on structure-solubility relationships is proposed in Appendix A.

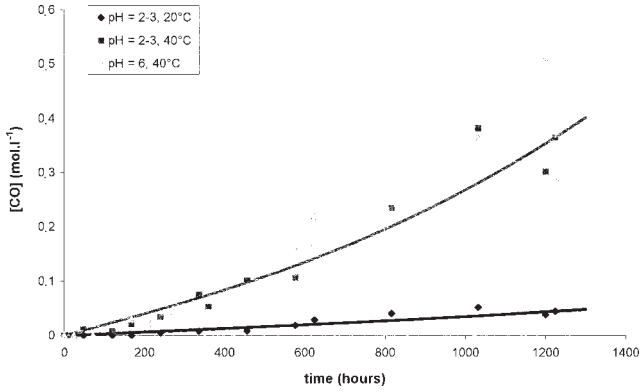

FIG. 6. Kinetic curves of carbonyl build-up of PE films after immersion in 80–90 ppm DOC solutions at 20 or 40°C and pH = 2–3 or 6. Comparison between the experimental results (points) and the model predictions (continuous lines) from *Eq. B6*.

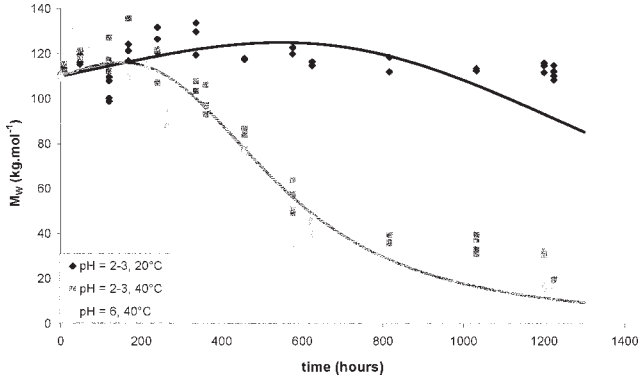

FIG. 7. Kinetic curves of weight average molar mass of PE films after immersion in 80–90 ppm DOC solutions at 20 or 40°C and pH = 2–3 or 6. Comparison between the experimental results (points) and the model predictions (continuous lines) from *Eq. B10*.

15482634, 2009, 7, Downloaded from https://4spepublications.onlinelibrary.wiley.com/doi/10.1002/pen.21258 by ENSAM, Wiley Online Library on [09/04/2025]. See the Terms and Conditions (https://onlinelibrary.wiley.com/terms-and-conditions) on Wiley Online Library for rules of use; OA articles are governed by the applicable Creative Commons License

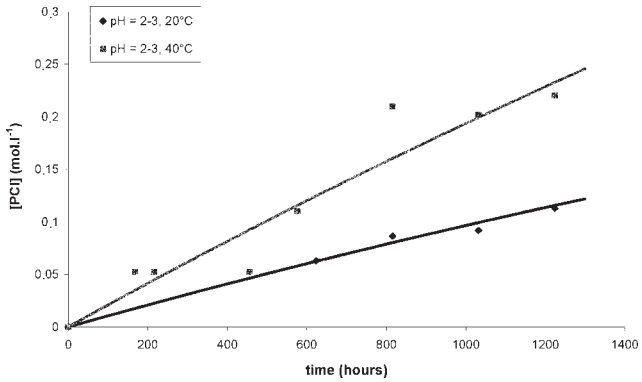

FIG. 8. Kinetic curves of chlorine concentration grafted to PE after immersion in 80–90 ppm DOC solutions at 20 or 40°C and pH = 2–3 or 6. Comparison between the experimental results (points) and the model predictions (continuous lines) from *Eq. B7*.

It leads to:

$$[\mathrm{DOC}]_{\mathrm{PE}} = \xi[\mathrm{DOC}]_{\mathrm{Water}} \tag{4}$$

where ξ is a constant almost temperature independent:

$$\xi = 1.5 \times 10^{-5}\ \mathrm{mol\,l^{-1}\,ppm^{-1}}\ \text{at}\ 20^{\circ}\mathrm{C}$$
$$\text{and}\ 1.7 \times 10^{-5}\ \mathrm{mol\,l^{-1}\,ppm^{-1}}\ \text{at}\ 40^{\circ}\mathrm{C};$$

$[\mathrm{DOC}]_{\mathrm{PE}}$ is the equilibrium DOC concentration in PE and $[\mathrm{DOC}]_{\mathrm{Water}}$ is the DOC concentration in water expressed in ppm.

As a radical, DOC can abstract hydrogen on phenolic antioxidants (AH) and on polyethylene (PH). In this latter case, it initiates radical chain oxidation. Oxygen can come from water but also from atmosphere by diffusion through the pipe wall. It will be considered here that oxygen dissolved in water is in equilibrium with atmosphere and that its concentration in PE obeys Henry's law:

$$[\mathrm{O_2}]_{\mathrm{equ}} = S\,p_{\mathrm{O_2}}, \tag{5}$$

with $S = 1.8 \times 10^{-8}$ mol l^{-1} Pa^{-1} [10].

As $p_{\mathrm{O_2}} = 2.1 \times 10^{4}$ Pa, then $[\mathrm{O_2}]_{\mathrm{equ}} = 3.8 \times 10^{-4}$ mol l^{-1}.

In the case of less oxygenated water, one would have:

$$\frac{[\mathrm{O_2}]_{\mathrm{PE}}}{[\mathrm{O_2}]_{\mathrm{equ}}} = \frac{[\mathrm{O_2}]_{\mathrm{Water}}}{[\mathrm{O_2}]_{\mathrm{Water\,equ}}}. \tag{6}$$

Radical chain oxidation leads to the formation of hydroperoxides (POOH) among other reaction products. As DOC is in relatively low concentration in PE and as its reactivity with PE is relatively low, the oxidation rate remains low as long as hydroperoxides are stable. At $T \leq 40^{\circ}$C, unimolecular POOH decomposition is extremely slow, its rate constant is of the order of 8×10^{-12} s^{-1} at 40°C. But, if the POOH concentration reaches a critical value of the order of 3×10^{-3} mol kg^{-1}, then hydroperoxides decompose bimolecularly, which induces a strong acceleration.

An interesting characteristic of this aging process is illustrated by the comparison of sample characteristics after 1200 h of exposure:

At 40°C, $s = (11 \pm 1) \times 10^{-2}$ mol l^{-1}
$[\mathrm{C{=}O}] = (40 \pm 10) \times 10^{-2}$ mol l^{-1},
At 20°C, $s \sim 0$ $[\mathrm{C{=}O}] = 5 \times 10^{-2}$ mol l^{-1}.

These results call for the following comments:

Each chain scission is probably accompanied by carbonyl formation because it results essentially from β scission of alkoxy radicals. However, there are almost four times more carbonyls than chain scissions that shows the existence of chemical events forming carbonyls without chain scission. The first mechanism which comes in mind is the Russel's termination one [11]:

$$>\mathrm{CH{-}OO^{\circ}} + {}^{\circ}\mathrm{OO{-}CH<} \rightarrow >\mathrm{C{=}O} + \mathrm{HO{-}CH<} + \mathrm{O_2}.$$

If the number of chain scissions was proportional to the number of carbonyls, it would be $\sim 14 \times 10^{-2}$ mol l^{-1} at 20°C, that would correspond to $M_{\mathrm{W}} = 66$ kg mol^{-1}, against 109 kg mol^{-1} for the initial value. Such a change would be easily observable. The fact that no change was observed at 20°C after 1200 h indicates thus that the mechanism of chain scission has not been activated at this temperature. A possible reason is that chain scission results essentially from hydroperoxide decomposition and that the critical value of hydroperoxide concentration, above which bimolecular decomposition becomes predominant, has not been reached after 1200 h at 20°C.

Hydroperoxide decomposition generates alkoxy radicals, which are precursors of chain scission, and its activation energy is relatively high ($\sim$100 kJ mol^{-1}) that can explain the difference between exposures at 40 and 20°C. Indeed, if the proposed mechanism is valid, one would expect autoacceleration and chain scissions after a certain exposure time (longer than 1200 h) at 20°C, because hydroperoxides also accumulate at this temperature.

Concerning the embrittlement process, it has been recently found that PE becomes brittle when its average molar mass M_{W} becomes lower than a critical value of the order of 70 ± 30 kg·mol^{-1} whatever its initial morphology [12]. Interpolation on the curve $M_{\mathrm{W}} = f(t)$ in Fig. 7 gives an embrittlement time of about 500 h at 40°C using $M_{\mathrm{W}} = 70$ kg mol^{-1} as an "endlife criterion." This value agrees with the experimental one, obtained from mechanical measurements and taking $\varepsilon_{\mathrm{R}} = 100\%$ as an "endlife criterion" (see Fig. 3). It appears thus that a kinetic model giving numbers s and x of chain scissions and crosslinks, i.e., allowing to calculate M_{W} at every exposure time, could be used to predict the embrittlement time using the above criterion.

15482634, 2009, 7, Downloaded from https://4spepublications.onlinelibrary.wiley.com/doi/10.1002/pen.21258 by ENSAM, Wiley Online Library on [09/04/2025]. See the Terms and Conditions (https://onlinelibrary.wiley.com/terms-and-conditions) on Wiley Online Library for rules of use; OA articles are governed by the applicable Creative Commons License

TABLE 1. Elementary reactions constituting the mechanistic scheme.

Code	Reaction	Rate constant
Iu	$POOH \rightarrow 2P^\circ + \gamma_{1S}\, s + \gamma_{1CO}\, CO$	k_{1u}
Ib	$2POOH \rightarrow P^\circ + PO_2^\circ + \gamma_{1S}\, s + \gamma_{1CO}\, CO$	k_{1b}
Id	$DOC + PH \rightarrow P^\circ + products$	k_{1d}
II	$P^\circ + O_2 \rightarrow PO_2^\circ$	k_2
III	$PO_2^\circ + PH \rightarrow POOH + P^\circ$	k_3
IV	$P^\circ + P^\circ \rightarrow$ inactive products $+ \gamma_4\, x$	k_4
V	$P^\circ + PO_2^\circ \rightarrow$ inactive products $+ (1 - \gamma_5)POOH + \gamma_5\, x$	k_5
VIa	$PO_2^\circ + PO_2^\circ \rightarrow Q + O_2$	k_{6a}
VIb	$Q \rightarrow POOP + x$	k_{6b}
VIc	$Q \rightarrow CO + P\text{–}OH$	k_{6c}
VId	$Q \rightarrow 2P^\circ + 2\gamma_{1S}\, s + 2\gamma_{CO}\, CO$	k_{6d}
VII	$P^\circ + DOC \rightarrow$ products (P—Cl)	k_7

The presence of chlorine grafted to the polymer in aged samples can be tentatively attributed to the combination of DOC with alkyl radicals to give organic chlorites:

$$O{=}Cl{-}O^\circ + P^\circ \rightarrow O{=}Cl{-}O{-}P.$$

As DOC induces PE oxidation, as shown by the build-up of hydroxyl and carbonyl groups, the nucleus of the mechanistic scheme must be the same as for thermooxidation. We have chosen to use the scheme recently established for PE thermooxidation at low temperature [13], to which both reactions involving DOC have been added (Table 1). The mechanistic scheme calls for following comments:

Reactions of P° radicals cannot be ignored because, in the following, the scheme will be applied to thick samples (the pipe wall) in which oxidation and DOC attack are diffusion controlled.

Crosslinking occurs through radical combinations, which are a mode of termination among others (for instance disproportionation). The yield of crosslinking is 0.50 for termination IV and 0.0108 for termination V at 40°C. Crosslinking occurs also in termination VI (see later).

In termination, it has been chosen to differentiate the distinct elementary processes, which leaded to consider four reactions (VIa–VId). Q is the caged pair of alkoxy radicals:

$$\text{(VIa)}\quad PO_2^\circ + PO_2^\circ \rightarrow [PO^\circ \quad PO^\circ]_{cage} + O_2, \quad (k_{6a})$$

$$\text{(VIb)}\quad [PO^\circ \quad OP^\circ]_{cage} \rightarrow POOP, \quad (k_{6b})$$

$$\text{(VIc)}\quad [PO^\circ \quad OP^\circ]_{cage} \rightarrow CO + P{-}OH, \quad (k_{6c})$$

$$\text{(VId)}\quad [PO^\circ \quad OP^\circ]_{cage} \rightarrow 2P^\circ + \text{inactive products}. \quad (k_{6d})$$

As it has been shown before [13], a part of alkoxy radicals escape from the cage (reaction VId) to initiate new radical chains and to give chain scissions.

Elementary rate constants k_{1u}, k_{1b}, k_2, k_3, k_4, k_5, k_{6a}, k_{6b}, k_{6c}, and k_{6d} have been previously determined [13] and will be used here without modification. Only k_5 has been slightly modified to improve the quality of the simulation. Their Arrhenius parameters and their values at 40°C are given in Table 2.

The Arrhenius parameters of reactions k_{1d} and k_7 (i.e., DOC reactions) can be considered as preliminary estimations, which need further checking. As a matter of fact, they were determined from only two points (at 40°C and 20°C), among which one (20°C) was obtained from incomplete data (exposure stopped before the end of the induction period). It can be considered that rate constant

TABLE 2. Arrhenius parameters and values at 40°C of kinetic parameters (rate constants and yields) for kinetic modeling.

Kinetic parameter	Pre-exponential factor (l mol^{-1} s^{-1} or s^{-1})	Activation energy (kJ mol^{-1})	Value at 40°C
k_{1u}	8.0×10^{12}	140	3.6×10^{-11}
k_{1b}	2.8×10^{9}	105	8.6×10^{-9}
k_{1d}	2.7×10^{-5}[a]	0[a]	2.7×10^{-5}
k_2	10^8	0	10^8
k_3	1.5×10^{10}	73	10^{-2}
k_4	8.0×10^{11}	0	8.0×10^{11}
k_5	1.5×10^{12}	5.9	1.6×10^{11}
k_{6a}	4.9×10^{19}	80	2.2×10^{6}
k_{6b}	2.0×10^{6}	0	2.0×10^{6}
k_{6c}	1.2×10^{6}	5	1.8×10^{5}
k_{6d}	4.8×10^{9}	17.4	6.0×10^{6}
k_7	6.6×10^{9}[a]	21.1[a]	2.0×10^{6}
γ_{1S}	—	—	100%
γ_{1CO}	—	—	70%
γ_4	—	—	50%
γ_5	—	—	1.08%

[a] Values carrying relatively high uncertainty.

15482634, 2009, 7, Downloaded from https://4spepublications.onlinelibrary.wiley.com/doi/10.1002/pen.21258 by ENSAM, Wiley Online Library on [09/04/2025]. See the Terms and Conditions (https://onlinelibrary.wiley.com/terms-and-conditions) on Wiley Online Library for rules of use; OA articles are governed by the applicable Creative Commons License

TABLE 3. Initial concentrations of chemical species at 40°C for kinetic modeling.

Chemical species	Initial concentration (mol l^{-1})
P°	0
PO_2°	0
POOH	10^{-2}
Q	0
PH	60
CO	0
P—Cl	0
x	0
s	0

values at 40°C are correct but that the values determined at 20°C are susceptible of modification.

The activation energy of the termination rate constant k_{6a} can appear surprisingly high. It is probably due to the fact that, for species in low concentration such as peroxy radicals, bimolecular reactions are diffusion controlled. Activation energy is lower for termination involving P° radicals because these latter migrate faster through valence migration:

$$P^\circ + PH \rightarrow PH + P^\circ.$$

The yield parameters γ_i correspond to the following processes:

γ_{1S} (= 1.0 at 40°C) is the yield of chain scissions from an alkoxy radical in reactions Iu, Ib, or VId. Chain scission is eventually in competition with hydrogen abstraction.

γ_{1CO} (= 0.70 at 40°C) is the yield of carbonyls from an alkoxy radical. In fact, each chain scission involves the formation of a carbonyl (an aldehyde in the case of PE):

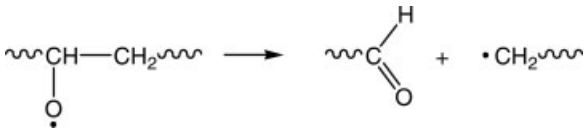

whereas each termination VIc gives a ketone.

The fact that γ_{1CO} differs from γ_{1s} comes from the fact that the contribution of aldehydes to the peak at 1720 cm^{-1} differs from the one of ketones. But, for the sake of simplicity, only one carbonyl species was considered in the calculation.

The DOC rate constants: k_{1d} and k_7 are determined from the above reported experimental data and the kinetic model (Appendix B) using an inverse approach [14].

The initial conditions are listed in Table 3.

The set of differential equations derived from the mechanistic scheme of Table 1 is presented in Appendix B. The measurable quantities [CO], M_W and [P—Cl] are calculated and plotted in Figs. 6–8. One can observe an apparently good simulation-experiment agreement, except perhaps for kinetic curves of M_W at 20°C (see Fig. 7) for which the amplitude of M_W changes over the whole time of exposure is too small relatively to the experimental standard deviation, to permit the determination of a correlation coefficient. Despite that, one can remark that the maximum gap between the simulated curve and the experimental points is not higher than 20%. On the contrary, at 40°C, the amplitude of M_W changes is high enough to permit the determination of the correlation coefficient: $R = 0.9390$.

For a so complex model, this set of three curves (at 40°C and 20°C) cannot be considered as a rigorous proof of the model validity, but it must be recalled that the major part of the model (all reactions except DOC ones) has been validated elsewhere [13].

Concerning DOC reactions, their rate constant values call for the following comments.

DOC is considerably less reactive than PO_2° radicals as well in hydrogen abstraction to PE: $k_{1d}/k_3 \approx 10^{-3}$, as in terminations: $k_7/k_5 = 10^{-3}$, where k_5 corresponds to the combination:

$$PO_2^\circ + P^\circ \rightarrow POOP.$$

The "extrinsic initiation" induced by DOC is relatively slow, but it is sufficient to induce catastrophic acceleration of the oxidation process in less than 500 h at 40°C.

As phenolic stabilizers are at least 1000 times more reactive than polyethylene in hydrogen abstractions, one can expect a fast antioxidant consumption by DOC attack.

Indeed, to be used for PE pipes, the kinetic model elaborated here must be completed by antioxidant reactions and by equations taking into account the reaction-diffusion coupling. These aspects will be studied in the second part of this article.

CONCLUSION

Aging of polyethylene (PE) films in highly concentrated (80–100 ppm) chlorine dioxide (DOC) solutions at 20 and 40°C for durations up to 1200 h has been studied by IR spectrophotometry, tensile testing, melt rheometry, and grafted chlorine titration. IR revealed a carbonyl growth indicating that DOC induces PE oxidation. Rheometry revealed the predominance of chain scissions, presumably linked to hydroperoxide decomposition. Tensile testing revealed an embrittlement process when the weight average molar mass M_W approaches a critical value of 70 kg mol^{-1}, which agrees with a previous study of PE thermooxidation. The kinetic model established in this latter study, completed with DOC elementary reactions with the polymer, has been used to try to simulate PE aging. The model agrees with experimental results obtained at 40°C and 20°C for all the studied characteristics. This model could appear exaggeratedly complex,

15482634, 2009, 7, Downloaded from https://4spepublications.onlinelibrary.wiley.com/doi/10.1002/pen.21258 by ENSAM, Wiley Online Library on [09/04/2025]. See the Terms and Conditions (https://onlinelibrary.wiley.com/terms-and-conditions) on Wiley Online Library for rules of use; OA articles are governed by the applicable Creative Commons License

TABLE 4. Molar mass (M), boiling point (T_b), critical temperature (T_{cr}), vaporization enthalpy (ΔH_V), ratio $\Delta H_V/RT_b$, and Lennard–Jones temperature (T_{LJ}).

Compound	M (g mol^{-1})	T_b (K)	T_{cr} (K)	ΔH_V (J mol^{-1})	$\Delta H_V/RT_b$	T_{LJ} (K)
SO_2	64.0	263	431	24.8	11.3	335
ClO_2	67.5	284	426	27.3	11.5	369

All the characteristics except T_{LJ} (ClO_2) were taken from Handbooks.

considering the monotony of experimental kinetic curves [except for $M_W = f(t)$ ones], and it could be tempting to try to reduce the mechanistic scheme to a single rate determining process.

However, in the case of such degenerate branching processes displaying an induction period and a strong autoaccelerated behavior, there is no way, to our opinion, to distinguish a rate determining elementary process. All the reactions play a key role.

The model will find its full usefulness in Part II of this article where antioxidant reactions and diffusion-reaction coupling will be added.

APPENDIX A: TRANSPORT PROPERTIES OF DOC

Transport properties of DOC in PE have never been studied to our knowledge. But, the properties of DOC are close to the ones of sulfur dioxide (Table 4), which can be used to estimate some DOC key characteristics, for instance the Lennard-Jones temperature T_{LJ}:

$$TLJ = \varepsilon/k, \tag{A1}$$

where ε is prefactor of the Lennard-Jones potential and k the Boltzmann constant.

T_{LJ} (SO_2) is known. It will be assumed that:

$$T_{LJ}(\mathrm{DOC}) = \mathrm{T_{LJ}}(SO_2)\frac{\Delta \mathrm{HV(DOC)}}{\Delta \mathrm{HV}(SO_2)}, \tag{A2}$$

where ΔH_V is the vaporization enthalpy.

One sees that the cohesive properties of ClO_2 are very close to SO_2 ones.

The solubility of DOC in PE will be calculated from the empirical equation established by Van Amerongen [15] and used, in the case of PE, by Michaels and Bixler [16]:

$$\log S(298\,K) = -7.0 + 0.010\,T_{LJ} \quad (S \text{ in cm}^3\ \text{STP cm}^{-3}\ \text{Pa}^{-1}) \tag{A3}$$

So that $S(298\ \mathrm{K}) = 2.2 \times 10^{-2}$ mol m^{-3} Pa^{-1} in amorphous phase.

For a sample of crystallinity ratio X_C, one can write:

$$S(298\,K) = 2.2 + 10^{-2}(1 - XC) \quad \text{in mol m}^{-3}\,\text{Pa}^{-1}. \tag{A4}$$

The same authors gave for the dissolution enthalpy H_S:

$$\frac{HS}{R} = 1000 - 10\,T_{LJ} \pm 500 = -2690 \pm 500\,\mathrm{K} \tag{A5}$$

ClO_2 dissolution in PE would be exothermic, so that the solubility would be a decreasing function of temperature:

$$S = S_0 \exp -\frac{HS}{\mathrm{RT}} \tag{A6}$$

with $S_0 = 2.6 \times 10^{-9}$ mol l^{-1} Pa^{-1} and $H_S/R = 2690$ K.

In the temperature interval of practical interest (20–40°C), S would keep the same order of magnitude.

To determine the DOC concentration in PE, we need to know the DOC partial pressure p in atmosphere, in equilibrium with the water solution. According to the water–DOC equilibrium diagram [17], one would have:

$$p = 11 \times 10^{-2}\ [\mathrm{DOC}]_{\mathrm{Water}} \text{ at } 20^\circ\mathrm{C}, \quad \text{and} \quad p = 22 \times 10^{-2}\ [\mathrm{DOC}]_{\mathrm{Water}} \text{ at } 40^\circ\mathrm{C},$$

where p is in Pa and $[\mathrm{DOC}]_{\mathrm{Water}}$ is the DOC weight fraction in water, expressed in ppm.

It can be assumed that p obeys Arrhenius law:

$$p = p_0 \exp -\frac{Ep}{\mathrm{RT}} \tag{A7}$$

with $p_0 = 5.7 \times 10^{-4}$ Pa ppm^{-1} and $E_p = 26.44$ kJ mol^{-1}.

Finally, the equilibrium DOC concentration in PE would be given by:

$$[\mathrm{DOC}] = [\mathrm{DOC}]_0 \exp -\frac{\mathrm{HD}}{\mathrm{RT}} \quad ([\mathrm{DOC}] \text{ in mol l}^{-1}) \tag{A8}$$

where $[\mathrm{DOC}]_0 = S_0\,p_0\,[\mathrm{DOC}]_{\mathrm{Water}} = 8.1 \times 10^{-5}\,[\mathrm{DOC}]_{\mathrm{Water}}$ ($[\mathrm{DOC}]_{\mathrm{Water}}$ in ppm) and $H_D = H_S + H_p = 4.06$ kJ mol^{-1}.

Thus, it comes:

$$[\mathrm{DOC}] = 1.4 \times 10^{-3}\ \text{mol l}^{-1} \quad \text{at 20 and 40°C}$$

for a DOC concentration in water of 80–90 ppm.

APPENDIX B: KINETIC MODEL

The kinetic model is the system of differential equations derived from the chosen mechanistic scheme (in Table 1). This system is composed of differential equations corresponding to the reactive species, plus the equations allowing to compute the measurable quantities such as the

DOI 10.1002/pen

15482634, 2009, 7, Downloaded from https://4spepublications.onlinelibrary.wiley.com/doi/10.1002/pen.21258 by ENSAM, Wiley Online Library on [09/04/2025]. See the Terms and Conditions (https://onlinelibrary.wiley.com/terms-and-conditions) on Wiley Online Library for rules of use; OA articles are governed by the applicable Creative Commons License

concentration of carbonyl groups, the number of chain scissions, the number of crosslinks, the number of chlorine atoms grafted to the polymer, and the whole oxygen quantity grafted to the polymer.

These equations are:

$$\frac{d[\mathrm{P}^\circ]}{dt} = 2k_{1u}[\mathrm{POOH}] + \mathrm{k}_{1b}[\mathrm{POOH}]^2 + \mathrm{k}_{1d}[\mathrm{DOC}][\mathrm{PH}] - k_2[\mathrm{O}_2][\mathrm{P}^\circ] + \mathrm{k}_3[\mathrm{PH}][\mathrm{PO}_2^\circ - 2\mathrm{k}_4[\mathrm{P}^\circ]^2 - k_5[\mathrm{P}^\circ]\mathrm{PO}_2^\circ] + 2\mathrm{k}_{6d}[\mathrm{Q}] - \mathrm{k}_7[\mathrm{P}^\circ][\mathrm{DOC}] \quad \text{(B1)}$$

$$\frac{d[\mathrm{PO2}^\circ]}{dt} = k_{1b}[\mathrm{POOH}]^2 + \mathrm{k}_2[\mathrm{O}_2][\mathrm{P}^\circ] - \mathrm{k}_3[\mathrm{PH}][\mathrm{PO}_2^\circ] - k_5[\mathrm{P}^\circ]\mathrm{PO}_2^\circ] - 2\mathrm{k}_{6a}[\mathrm{PO}_2^\circ]^2 \quad \text{(B2)}$$

$$\frac{d[\mathrm{POOH}]}{dt} = -k_{1u}[\mathrm{POOH}] - 2\mathrm{k}_{1b}[\mathrm{POOH}]^2 + \mathrm{k}_3[\mathrm{PH}][\mathrm{PO}_2^\circ] + (1-\gamma_5)k_5[\mathrm{P}^\circ][\mathrm{PO}_2^\circ], \quad \text{(B3)}$$

$$\frac{d[\mathrm{Q}]}{dt} = k_{6a}[\mathrm{PO}_2^\circ] - (\mathrm{k}_{6b} + \mathrm{k}_{6c} + \mathrm{k}_{6d})[\mathrm{Q}] \quad (\mathrm{Q} = \text{caged pair of PO}^\circ \text{ radicals}), \quad \text{(B4)}$$

$$\frac{d[\mathrm{PH}]}{dt} = -(2+\gamma_{1S})k_{1u}[\mathrm{POOH}] - (1+\gamma_{1S})\mathrm{k}_{1b}[\mathrm{POOH}]^2 - k_{1d}[\mathrm{DOC}][\mathrm{PH}] - \mathrm{k}_3[\mathrm{PH}][\mathrm{PO}_2^\circ] + 2\gamma_4\mathrm{k}_4[\mathrm{P}^\circ]^2 + (3\gamma\mathrm{s}-1) \times k_5[\mathrm{P}^\circ][\mathrm{PO}_2^\circ] + 2\mathrm{k}_{6b}[\mathrm{Q}] - 2(1+\gamma_{1S})\mathrm{k}_{6d}[\mathrm{Q}], \quad \text{(B5)}$$

$$\frac{d[\mathrm{CO}]}{dt} = \gamma_{1CO}k_{1u}[\mathrm{POOH}] + \gamma_{1CO}\mathrm{k}_{1b}[\mathrm{POOH}]^2 + \mathrm{k}_{6c}[\mathrm{Q}] + 2\gamma_{1CO}k_{6d}[\mathrm{Q}], \quad \text{(B6)}$$

$$\frac{d[\mathrm{PCl}]}{dt} = k_7[\mathrm{P}^\circ][\mathrm{DOC}], \quad \text{(B7)}$$

$$\frac{ds}{dt} = \gamma_{1S}k_{1u}[\mathrm{POOH}] + \gamma_{1S}\mathrm{k}_{1b}[\mathrm{POOH}]^2 + 2\gamma_{1S}\mathrm{k}_{6d}[\mathrm{Q}] \quad \text{(B8)}$$

$$\frac{dx}{dt} = \gamma 4k_4[\mathrm{P}^\circ]^2 + \gamma 5\mathrm{k}_5[\mathrm{P}^\circ][\mathrm{PO}_2^\circ] + \mathrm{k}_{6d}[\mathrm{Q}], \quad \text{(B9)}$$

$$\frac{1}{Mw} - \frac{1}{M_{w0}} = \frac{s}{2} - 2x \quad \text{(B10)}$$

The method of resolution of this system of equations has been already described [14]. Very briefly, it is based on implicit or semi-implicit algorithms dedicated to stiff systems of differential equations. These algorithms give a satisfying approximate solution for a reasonable cost of calculation. The results reported in this study were obtained applying the ODE23s solver of Matlab software [18], based on the semi-implicit Rosenbrock's algorithm. The resolution gave access to the kinetic curves of reactive and inactive species concentrations.

REFERENCES

1. Y. Lu and N. Brown, *J. Mater. Sci.*, **25**, 29 (1990).
2. C.J.G. Plummer, "Microdeformation and Fracture in Semicrystalline Polymers," in *Mechanical Properties of Polymers Based on Nanostructure and Morphology, Chap. 6*, G.H. Michler and F.-J.B. Calleja, Eds., CRC Press, New York, 216 (2005).
3. J. Viebke, E. Elble, M. Ifwarson, and U.W. Gedde, *Polym. Eng. Sci.*, **34**(**17**), 1354 (1994).
4. U.W. Gedde, J. Viebke, H. Leijstrom, and M. Ifwarson, *Polym. Eng. Sci.*, **34**, 1773 (1994).
5. J. Viebke, M. Hedvenquist, and U.W. Gedde, *Polym. Eng. Sci.*, **36**, 2896 (1996).
6. J. Viebke and U.W. Gedde, *Polym. Eng. Sci.*, **37**(**5**), 896 (1997).
7. J.P. Dear and N.S. Mason, *Polym. Polym. Comp.*, **9**, 1 (2001).
8. J. Hassinen, M. Lundback, M. Ifwarson, and U.W. Gedde, *Polym. Deg. Stab.*, **84**, 261 (2000).
9. O. Saito, *J. Phys. Soc. Japan.*, **13**, 1451 (1967).
10. D.W. Van Krevelen and P.J. Hoftyzer, *Properties of Polymers. Their Estimation and Correlation with Chemical Structure*, *2nd Edition*, Amsterdam, Elsevier, 406 (1976).
11. G.A. Russel, *J. Am. Chem. Soc.*, **79**, 3871 (1957).
12. N. Khelidj, X. Colin, L. Audouin, and J. Verdu, *Nuclear Instr. Methods in Phys. Res.*, **B236**, 94 (2005).
13. N. Khelidj, X. Colin, L. Audouin, J. Verdu, C. Monchy-Leroy, and V. Prunier, *Polym. Deg. Stab.*, **91**(**7**), 1593 (2006).
14. X. Colin, L. Audouin, and J. Verdu, *Polym. Deg. Stab.*, **86**, 309 (2004).
15. G.J. Van Amerongen, *Rubb. Chem. Technol.*, **37**, 1065 (1964).
16. A.S. Michaels and H.J. Bixler, *J. Polym. Sci.*, **50**, 383, 413 (1961).
17. Anonymous, *La Tribune de L'eau* (France), **613–614**, 12 (Sept–Dec 2001).
18. Matlab, *The Language of Technical Computing, Version 6*, The MathWorks, Inc., Natick (2000).

15482634, 2009, 7, Downloaded from https://4spepublications.onlinelibrary.wiley.com/doi/10.1002/pen.21258 by ENSAM, Wiley Online Library on [09/04/2025]. See the Terms and Conditions (https://onlinelibrary.wiley.com/terms-and-conditions) on Wiley Online Library for rules of use; OA articles are governed by the applicable Creative Commons License